ANL/NE-12/61

Verification Test Suite for Systems Analysis Tools

Nuclear Engineering Division

About Argonne National Laboratory

Argonne is a U.S. Department of Energy laboratory managed by UChicago Argonne, LLC under contract DE-AC02-06CH11357. The Laboratory's main facility is outside Chicago, at 9700 South Cass Avenue, Argonne, Illinois 60439. For information about Argonne, see http://www.anl.gov.

Availability of This Report

This report is available, at no cost, at http://www.osti.gov/bridge. It is also available on paper to the U.S. Department of Energy and its contractors, for a processing fee, from:

U.S. Department of Energy
Office of Scientific and Technical Information
P.O. Box 62
Oak Ridge, TN 37831-0062
phone (865) 576-8401
fax (865) 576-5728
reports@adonis.osti.gov

Disclaimer

This report was prepared as an account of work sponsored by an agency of the United States Government. Neither the United States Government nor any agency thereof, nor UChicago Argonne, LLC, nor any of their employees or officers, makes any warranty, express or implied, or assumes any legal liability or responsibility for the accuracy, completeness, or usefulness of any information, apparatus, product, or process disclosed, or represents that its use would not infringe privately owned rights. Verification herein to any specific commercial product, process, or service by trade name, trademark, manufacturer, or otherwise, does not necessarily constitute or imply its endorsement, recommendation, or favoring by the United States Government or any agency thereof. The views and opinions of document authors expressed herein do not necessarily state or reflect those of the United States Government or any agency thereof, Argonne National Laboratory, or UChicago Argonne, LLC.

ANL/NE-12/61

Verification Test Suite for Systems Analysis Tools

T. Sumner, R. Hu, and T. H. Fanning
Nuclear Engineering Division
Argonne National Laboratory

December 21, 2012

ABSTRACT

This report documents strategies and test problems to support Verification and Validation (V&V) of the systems analysis tools currently being developed under the Reactor Product Line (RPL) of DOE's Nuclear Energy Advanced Modeling and Simulation (NEAMS) program. A suite of verification test cases has been developed. This test suite supports development of new codes as well as maintenance of existing codes. For advanced tools that are under development like RELAP-7 for light water reactor analysis [1] and the MOOSE-based component models for SFR (M-SFR) analyses [2], verification of simulation results must be performed throughout the entire development phase. This test suite is also useful for established codes as part of automated testing to ensure that general code maintenance does not change existing results.

The tests that have been completed focus on calculating fuel and cladding temperature and coolant temperature and pressure. Analytical solutions to many of the tests have been provided to confirm code predictions. For tests where full analytical solutions are not available numerical approximations have been created for comparison with code results.

Each of the test cases have been evaluated with SAS4A/SASSYS-1 [4]. The results of these tests compared very well with the analytical and numerical solutions, with maximum temperature differences on the order of 0.013 K for each test. Many of the tests were also evaluated with M-SFR. The M-SFR predictions compared well to the analytical results. The biggest differences between analytical and M-SFR results were in the fuel-cladding gap ΔT and the fuel centerline temperature with differences on the order of 2 K. For the fuel centerline temperatures, the error was due to the use of a linear finite element method to solve the heat conduction equation. Future updates to the code will likely improve this approximation.

This effort will continue as the tests described above are expanded to address other areas of systems analyses. These will include the primary and intermediate cooling systems and balance of plant. As it evolves, this test suite will cover the full range of sodium fast reactor conditions including challenging coupled multi-physics challenge problems.

TABLE OF CONTENTS

Abstract ii

Table of Contents iii

1 Introduction 1

2 Base Case 2

2.1 Definition 2
2.2 Analytical Solution for Temperature 3
2.3 Analytical Solution for Pressure 7

3 Additional Test Cases 8

3.1 Simple Base Case Extensions 8
3.1.1 Increasing the Number of Fuel Pins 8
3.1.2 Increasing the Number of Subassemblies 8
3.1.3 Subassemblies with Different Power Production 9
3.1.4 Introduction of a Fission Gas Plenum 10
3.1.5 Introduction of Reflectors Above and Below the Core 10
3.2 Simple Transient Cases 11
3.2.1 Increased Simulation Time 11
3.2.2 Increased Reactor Power 11
3.2.3 Increased Core Inlet Temperature 12
3.2.4 Decreased Sodium Mass Flow Rate 12
3.3 Temperature-dependent Material Properties 13
3.3.1 Sodium Heat Capacity 13
3.3.2 Cladding Thermal Conductivity 14
3.3.3 Fuel Thermal Conductivity 14
3.4 Neutron Kinetics Cases 14
3.4.1 Delayed Neutron Precursors 14
3.4.2 External Reactivity Insertion 15

4 Results of Verification Testing 16

4.1 Base case 16
4.2 Additional Test Case Results 20
4.2.1 Simple Base Case Extensions 20
4.2.2 Simple Transient Cases 21
4.2.3 Material Property Cases 21
4.2.4 Neutron Kinetics Cases 22

5 Future Test Cases 23

5.1 Neutronics Tests 23
5.2 Multi-Channel Test 23
5.3 Component Tests 24
5.4 Simple Loop Test 24
5.5 Full System Tests 25

6 Summary 25
References 26

1 Introduction

This report documents strategies and test problems to support the Verification and Validation (V&V) of the systems analysis tools currently being developed under the Reactor Product Line (RPL) of DOE's Nuclear Energy Advanced Modeling and Simulation (NEAMS) program. A suite of verification test cases has been developed. The problems contained in this test suite are designed for the verification of systems analysis codes in general but are targeted to the conditions of sodium cooled fast reactors (SFR). This test suite supports development of new codes as well as maintenance of existing codes. For advanced tools that are under development like RELAP-7 for light water reactor analysis [1] and the MOOSE-based component models for SFR (M-SFR) analyses [2], verification of simulation results must be performed throughout the entire development phase. This test suite is also useful for established codes as part of automated testing to ensure that general code maintenance does not change existing results.

Additional tests are being developed as part of on-going software quality assurance. The test suite will cover the full spectrum of systems analysis code capabilities and range from very simple steady-state single pin models to full system transients based loosely on documented fast reactor designs. The test suite uses a targeted code coverage approach by introducing small differences for each successive test in order to isolate specific areas of a code. By modeling tests with small differences, the effect of each additional modeling feature can be identified and compared with expected results.

Whenever possible, analytical solutions to a test case have been created. For some tests, however, analytical solutions are not possible or practical. As systems analysis tools evolve, code developers will be able to verify that they continue to predict the correct solution. For the tests without analytical solutions, numerical solutions were created for comparison with code results.

The tests that have been completed are documented below, beginning with a very simple steady-state single-pin problem for which analytical solutions for temperature and pressure are derived. All other tests in this test suite are derived from this base case. Results of many of the tests performed with two systems analysis codes are compared against the analytical solutions. These comparisons have already proven useful in identifying a small issue in the Moose-based SFR fuel-pin model. Because of the nature of the linear finite elements being used to solve for temperature, the fuel-pin model slightly under predicts peak fuel temperatures. This fuel pin model is also part of RELAP-7 so a similar error would be expected for LWR analyses.

Finally, areas of systems analysis codes to be addressed in future test cases are described. Future tests will address core flow distribution, primary and intermediate heat transport systems, and balance of plant among others.

2 Base Case

The starting point for code verification is to develop a base case that code developers can use to assess how well their tool predicts the most basic phenomena. From this base case, more complicated models will be defined. In this section, the definition of the verification test suite base case is given followed by the analytical temperature and pressure solutions. All other test cases described in this report are derived from this base case.

2.1 Definition

The base test case is a steady-state, single pin problem with uniform dimensions and constant properties. The fuel pin has a constant linear heat generation rate of 37.5 kW/m and the boundaries of the problem are set as the top and bottom of the fuel pin. Sodium coolant enters from the bottom at 0.15 kg/s and a temperature of 628.15 K and it leaves at the top of the pin at a pressure of 200,000 Pa. No wire wrap or subassembly hex can is defined for this problem. All necessary dimensions and sodium, cladding, and fuel properties are given in Table 2.1 below.

Table 2.1. Parameters of the Base Case

General		
# Pins	-	1
Coolant Inlet Temp	K	628.15
Mass Flow Rate Per Pin	kg/s	0.15
Total Power	W	30000
Pin Dimensions		
Fuel Height	m	0.8
Fuel Radius	m	3.01500E-03
Cladding Inner Radius	m	3.48000E-03
Cladding Outer Radius	m	4.00000E-03
Hydraulic Diameter	m	3.18310E-03
Coolant Flow Area	m^2	2.00000E-05
Wetted Perimeter	m	2.51327E-02
Thermo-Physical Properties		
Fuel Thermal Conductivity	W/m-K	16
Clad Thermal Conductivity	W/m-K	26
Gap Thermal Conductivity	W/m-K	64
Sodium Density	kg/m^3	800
Sodium Heat Capacity	J/kg-K	1260
Sodium Thermal Conductivity	W/m-K	60
Sodium Heat Transfer Coefficient	W/m^2-K	1.60E+05
Sodium Viscosity	Pa-s	2.00E-04
Other Values		
Friction Factor		0.017
Pressure at Core Outlet	Pa	2.00E+05

Thermal hydraulic parameters such as heat transfer coefficient and friction factor have been fixed to eliminate differences resulting from the choice of correlations. Code verification is considered successful if the model correctly predicts the axial temperature distributions at the following locations:

- Fuel centerline,
- Fuel surface,
- Cladding inner surface,
- Cladding outer surface, and
- Coolant.

Additionally, the axial pressure distribution within the sodium coolant channel should be predicted correctly.

2.2 Analytical Solution for Temperature

The axial temperature profile is solved analytically for the base case at several locations. Chapter 13 of Reference 3 solves for these axial temperature profiles for the case of a sinusoidal axial power production. A similar method is used in the solutions below but for a constant axial power profile.

Equation 2.1 presents a reduced form of the energy equation in a coolant channel at steady-state with constant flow area. The terms for pressure gradient and friction dissipation are neglected.

$$\dot{m}\frac{d}{dz}\,h_m = q'(z) \tag{2.1}$$

In this equation $\dot{m}$ is mass flow rate, h_m is specific enthalpy of the coolant, and $q'(z)$ is the linear heat generation rate. Integrating this equation over the axial length gives the following:

$$\dot{m}\int_{h_{\text{in}}}^{h_m(z)} dh_m = \int_0^z q'(z)\,dz \tag{2.2}$$

For a constant linear heat generation rate, $q'(z) = q'$, Equation 2.2 may be simplified to:

$$\dot{m}\,c_p\int_{T_{\text{in}}}^{T_m(z)} dT = q' \cdot z \tag{2.3}$$

where c_p is the specific heat capacity of the coolant and T_m is the coolant temperature and T_{in} equals $T_m(0)$.

For single-phase sodium flow, the coolant temperature solution is:

$$T_m(z) = T_{\text{in}} + \frac{q' \cdot z}{\dot{m}\, c_p} \tag{2.4}$$

The coolant temperature profile, along with the other temperature profiles derived below, is plotted for the base case in Figure 2.1.

Next the axial temperature profile at the outer cladding surface can be found by using a constant heat flux at that surface, as shown in Equation 2.5:

$$\mathrm{h_c}\left(T_{co}(z) - T_m(z)\right) = \mathrm{q''} = \frac{\mathrm{q'}}{\mathrm{P_h}} = \frac{\mathrm{q'}}{2\,\pi\,\mathrm{R_{co}}} \tag{2.5}$$

where R_{co} is the radius of the outer cladding surface and h_c is the sodium heat transfer coefficient. Combining Equations 2.4 and 2.5 and eliminating $T_m(z)$ results in:

$$T_{co}(z) = T_{\text{in}} + \mathrm{q'}\left(\frac{z}{\dot{m}\, c_p} + \frac{1}{2\,\pi\,\mathrm{R_{co}}\, h_c}\right) \tag{2.6}$$

Based on the heat conduction equation for cylindrical coordinates, the temperature drop across the cladding is

$$T_{\text{ci}} - T_{co} = \frac{q'}{2\,\pi\, k_c} \ln\left(\frac{R_{co}}{R_{ci}}\right) \tag{2.7}$$

where R_{ci} is the radius of the cladding inner surface and k_c is the thermal conductivity of the cladding. Combining Equations 2.6 and 2.7 and eliminating $T_{co}(z)$ leads to:

$$T_{ci}(z) = T_{\text{in}} + \mathrm{q'}\left(\frac{z}{\dot{m}\, c_p} + \frac{1}{2\,\pi\,\mathrm{R_{co}}\, h_c} + \frac{1}{2\,\pi\, k_c} \ln\left(\frac{R_{co}}{R_{ci}}\right)\right) \tag{2.8}$$

Next the fuel surface temperature can be found by calculating the temperature drop across the sodium gap. For a cylindrical fuel pin, this can be calculated in the same way as Equation 2.5:

$$\mathrm{h_g}\left(T_{fs}(z) - T_{ci}(z)\right) = \mathrm{q''} = \frac{\mathrm{q'}}{\mathrm{P_f}} = \frac{\mathrm{q'}}{2\,\pi\,\mathrm{R_f}} \tag{2.9}$$

where h_g is the heat transfer coefficient of the gap and R_f is the radius at the fuel outer surface. Combining Equations 2.8 and 2.9 and eliminating $T_{ci}(z)$ leads to Equation 2.10 for the fuel surface temperature.

$$T_{fs}(z) = T_{\text{in}} + \mathrm{q'}\left(\frac{z}{\dot{m}\, c_p} + \frac{1}{2\,\pi\,\mathrm{R_{co}}\, h_c} + \frac{1}{2\,\pi\, k_c} \ln\left(\frac{R_{co}}{R_{ci}}\right) + \frac{1}{2\,\pi\,\mathrm{R_f}\, h_g}\right) \tag{2.10}$$

Reference 3 presents a derivation where the steady-state heat conduction equation is solved for a cylindrical fuel pin to give:

$$\int_{T_{fs}}^{T_{CL}} k_f \, dT = \frac{\mathrm{q}''' R_{fo}^2}{4} \tag{2.11}$$

Because the linear heat rate q' at the fuel surface is $\pi \, \mathrm{q}''' R_{fo}^2$, Equation 2.11 reduces to:

$$\int_{T_{fs}}^{T_{CL}} k_f \, dT = \frac{\mathrm{q}'}{4\,\pi} \tag{2.12}$$

For a temperature-independent fuel thermal conductivity, Equation 2.12 can be further simplified to:

$$k_f (T_{CL} - T_{fs}) = \frac{\mathrm{q}'}{4\,\pi} \tag{2.13}$$

By combining Equations 2.10 and 2.13 and eliminating T_{fs}, the fuel centerline temperature can be found as:

$$T_{fs}(z) = T_{\mathrm{in}} + \mathrm{q}' \left(\frac{z}{\dot{m}\, c_p} + \frac{1}{2\,\pi\,\mathrm{R_{co}}\, h_c} + \frac{1}{2\,\pi\, k_c} \ln\left(\frac{R_{co}}{R_{ci}}\right) + \frac{1}{2\,\pi\,\mathrm{R_f}\, h_g} + \frac{1}{4\,\pi\, k_f} \right) \tag{2.14}$$

All data needed to calculate the analytical axial temperature profiles are given in Table 2.1. Because all properties are temperature-independent, the shape of the radial temperature profile is constant at all axial locations. The resulting axial temperature profiles corresponding to Equations 2.4, 2.6, 2.8, 2.10, and 2.14 are illustrated in Figure 2.1 and given in Table 2.2 at every 5 cm.

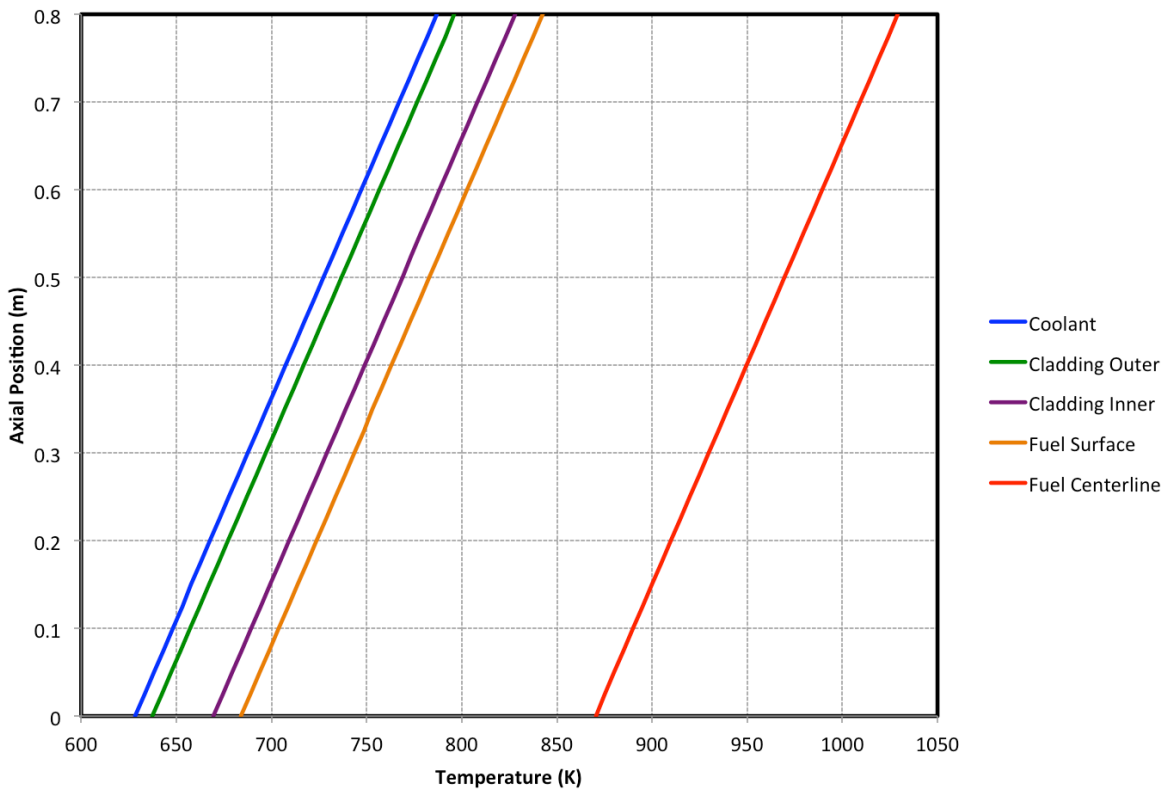

Figure 2.1. Axial Temperature Profile for Base Case

Table 2.2. Axial Temperature Profile for Base Case

Axial Position (m)	Coolant Temperature (K)	Cladding Outer Temperature (K)	Cladding Inner Temperature	Fuel Surface Temperature (K)	Fuel Centerline Temperature (K)
0.80	786.880	796.206	828.173	842.556	1029.066
0.75	776.960	786.285	818.253	832.635	1019.145
0.70	767.039	776.364	808.332	822.715	1009.224
0.65	757.118	766.444	798.411	812.794	999.304
0.60	747.198	756.523	788.491	802.873	989.383
0.55	737.277	746.602	778.570	792.953	979.462
0.50	727.356	736.682	768.649	783.032	969.542
0.45	717.436	726.761	758.729	773.111	959.621
0.40	707.515	716.841	748.808	763.191	949.701
0.35	697.594	706.920	738.888	753.270	939.780
0.30	687.674	696.999	728.967	743.350	929.859
0.25	677.753	687.079	719.046	733.429	919.939
0.20	667.833	677.158	709.126	723.508	910.018
0.15	657.912	667.237	699.205	713.588	900.097
0.10	647.991	657.317	689.284	703.667	890.177
0.05	638.071	647.396	679.364	693.746	880.256
0.00	628.150	637.475	669.443	683.826	870.335

2.3 Analytical Solution for Pressure

The analytical solution for the pressure drop through the coolant channel has two components: gravity pressure drop and friction pressure drop. For a flow channel with constant area and coolant density, there is no acceleration pressure drop. Equation 2.15 shows the equation for the gravity pressure drop at axial position z in the coolant channel.

$$\Delta p_{\text{grav}} = \int \rho_{\text{Na}} \cdot g \cdot dz = \rho_{\text{Na}} \cdot g \cdot (z_{\text{outlet}} - z) \tag{2.15}$$

The pressure drop due to friction is defined by:

$$\Delta p_{\text{fric}} = \int \frac{f\, v_m^2}{2 \cdot \rho_{\text{Na}} \cdot D_h \cdot A^2}\, dz = \frac{f\, v_m^2}{2 \cdot \rho_{\text{Na}} \cdot D_h \cdot A^2}\, (z_{\text{outlet}} - z) \tag{2.16}$$

Combining these two equations with the coolant outlet pressure, P_{outlet}, gives a coolant pressure distribution of:

$$p(z) = p_{\text{outlet}} + \left[\rho_{\text{Na}} \cdot g + \frac{f\, v_m^2}{2 \cdot \rho_{\text{Na}} \cdot D_h \cdot A^2}\right] \cdot (z_{\text{outlet}} - z) \tag{2.17}$$

Assuming a value of 9.8 $\frac{m}{s^2}$ for acceleration due to gravity and using the values given in Table 2.1, the individual pressure drop components and the pressure distribution in the coolant channel for the base case are given in Table 2.3 and Figure 2.2.

Table 2.3. Axial Coolant Pressure for Base Case

Axial Position (z)	Gravity ΔP (Pa)	Friction ΔP (Pa)	Coolant Pressure (Pa)
0.80	0	0	200000
0.75	392	9388	209780
0.70	784	18776	219560
0.65	1176	28164	229340
0.60	1568	37552	239120
0.55	1960	46940	248900
0.50	2352	56328	258680
0.45	2744	65716	268460
0.40	3136	75104	278240
0.35	3528	84492	288020
0.30	3920	93880	297800
0.25	4312	103268	307580
0.20	4704	112656	317360
0.15	5096	122044	327140
0.10	5488	131431	336919
0.05	5880	140819	346699
0.00	6272	150207	356479

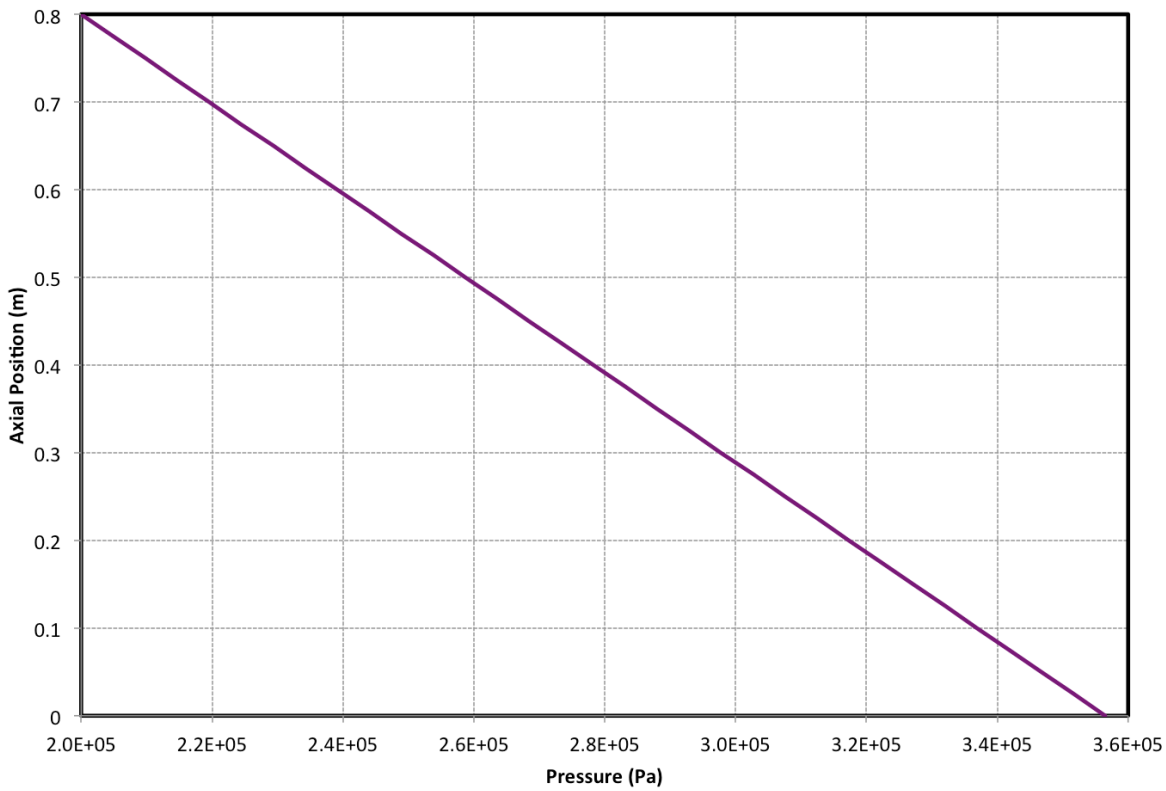

Figure 2.2. Axial Pressure Profile for Base Case

3 Additional Test Cases

Additional cases have been created that increase the complexity of the verification tests through incremental changes to the base case. By creating test cases with small changes, issues within a code can more quickly be identified if the code fails one test but not others. The cases defined below have been implemented and used to validate the solution methods of two systems analysis codes. The results for these codes are presented in the next section.

3.1 Simple Base Case Extensions

3.1.1 *Increasing the Number of Fuel Pins*

While the base case defines a single pin problem, systems analysis codes typically perform the same simulations for multiple pins. In this test case, the number of pins from the base case is increased from 1 to 91. Total power increases from 30 kW to 2730 kW. With the assumption that all 91 pins have the same geometry and power production, the reference temperature and pressure results are identical to the base case analytical solutions, which are given in Tables 2.2 and 2.3.

3.1.2 *Increasing the Number of Subassemblies*

Fuel pins in a reactor are usually grouped into a number of subassemblies. This test case defines a problem with 100 subassemblies and 91 pins per subassembly. The subassemblies and pins are identical with each pin being defined by the parameters given in Table 2.1. Total

power increases from 2730 kW in the preceding case to 273 MW. As with the previous test case, the pressure and temperature results for this test case are identical to those given in Tables 2.2 and 2.3.

3.1.3 *Subassemblies with Different Power Production*

This test case introduces a second pin type with identical geometry to the original pin type but different power production and coolant flow. By introducing a second pin type, this case verifies that code results are correctly predicting the temperature profile of the second pin type while also maintaining the correct solution to the original pin type.

In this test case, the geometry defined in Table 2.1 is assumed for both pins. The power production and coolant mass flow per pin are defined in Table 3.1. Because the power production and coolant flow rate for Pin Type #1 are identical to the base case, the temperatures for Pin Type #1 should be identical to those given in Table 2.2. The temperature profile for Pin Type #2, which is calculated in the same manner as detailed in Section 2.2, is illustrated in Figure 3.1.

Table 3.1. Power and Flow for Two-Pin Test Case

	Power per pin (kW)	Flow per pin (kg/s)
Pin Type #1	30.0	0.150
Pin Type #2	40.0	0.130

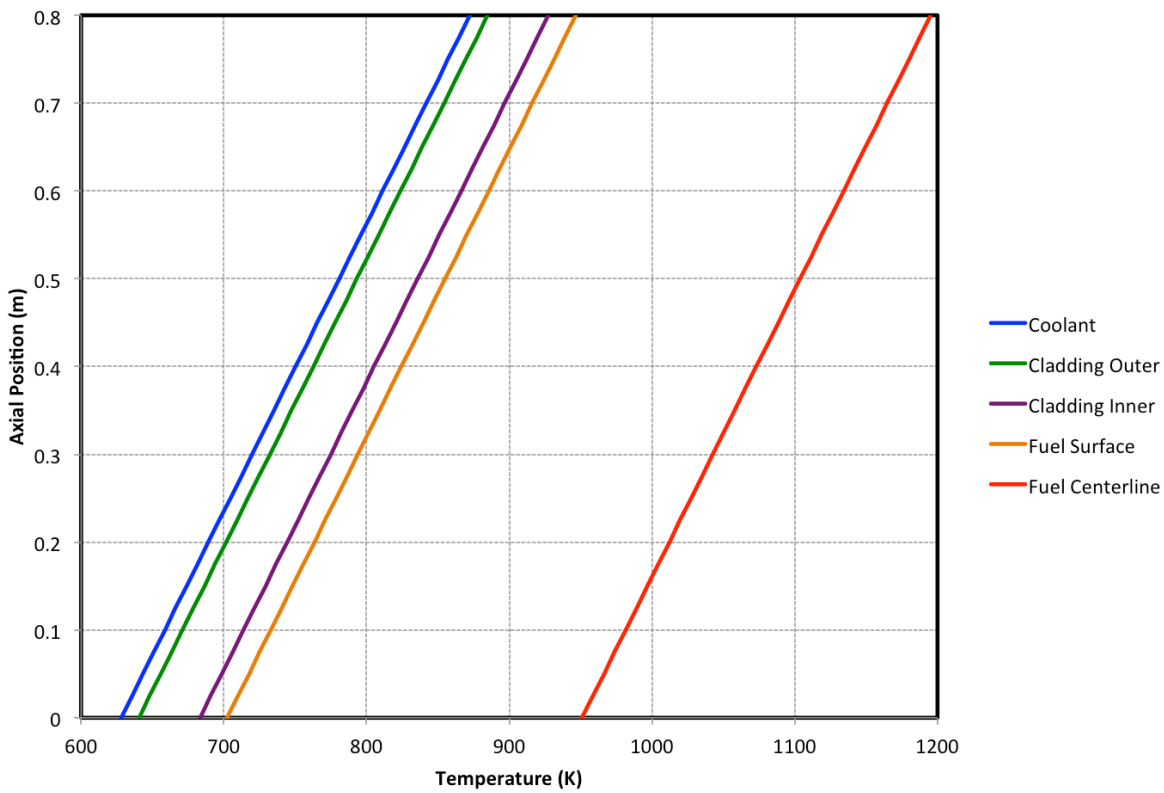

Figure 3.1. Axial Temperature Profile for Second Channel

3.1.4 *Introduction of a Fission Gas Plenum*

Fuel pins in SFRs usually have a fission gas plenum. This test introduces a 1.2-meter tall fission gas plenum to the problem defined for the base case. The dimensions of the coolant and cladding in the gas plenum region are identical to those given in Table 2.1. The space inside the cladding is filled with fission gas.

Assuming no axial conduction or power production in this region, the temperature for a fission gas plenum above the fuel should be constant at the coolant outlet temperature of 786.88 K. For systems codes that are capable of simulating a fission gas plenum below the fuel, the temperature throughout the gas plenum region should be constant at the coolant inlet temperature of 628.15 K. In both cases, the axial and radial temperature profile in the fuel pin should remain unchanged from the values given in Tables 2.2 and 2.3.

3.1.5 *Introduction of Reflectors Above and Below the Core*

This case is an extension of the single pin base case with axial reflectors introduced above and below the fueled region. This case is similar to the previous one in that the addition of a structure above or below the power-producing region should not result in any change in the temperatures calculated in the fuel region. The reflectors below the fuel should have a uniform temperature equal to the inlet temperature of 628.15 K while the reflectors above the fuel should have a uniform temperature equal to the outlet temperature of 786.88 K. The dimensions of the cylindrical upper and lower axial reflectors are identical and are

summarized in Table 3.3. As an additional note, material properties of the reflector pins should not affect the results.

Table 3.3. Parameters for Reflectors Test Case

	Lower Reflector	Upper Reflector
Flow Area (m^2)	2.0E-5	2.0E-5
Radius (m)	4.0E-3	4.0E-3
Wetted Perimeter (m)	2.51327E-2	2.51327E-2
Hydraulic Diameter (m)	3.18310E-3	3.18310E-3
Height (m)	1.0	1.0

3.2 Simple Transient Cases

All the cases above test various aspects of the steady-state solver for a systems analysis code. In the tests below, simple transient cases are defined to test the ability of a systems analysis code to equilibrate to a new steady-state solution following some change. Because analytical solutions of the temperatures during the transient are very difficult to calculate, only analytical solutions of the resulting equilibrium state are given. Predictions from systems analysis codes following the development of a new equilibrium state should be compared against these temperatures to confirm that the code can correctly equilibrate to a new steady-state. Each test is based off of the base case.

3.2.1 *Increased Simulation Time*

While the base case verifies that systems analysis codes are able to correctly solve for the steady-state solution to simple problems, they must also be able to maintain those solutions for a steady-state simulation. For this test case, the steady-state results from the base case should be compared with the results after 1000 seconds of simulation time. The results after 1000 seconds should still match those given in Tables 2.2 and 2.3.

3.2.2 *Increased Reactor Power*

In this test case, reactor power for the single fuel pin increases from 30 kW to 45 kW shortly after the start of the transient. Because each of the materials are defined with constant properties, the difference between all temperatures and the inlet temperature of 628.15 K should increase by exactly 50%. The resulting temperatures are illustrated in Figure 3.2 below.

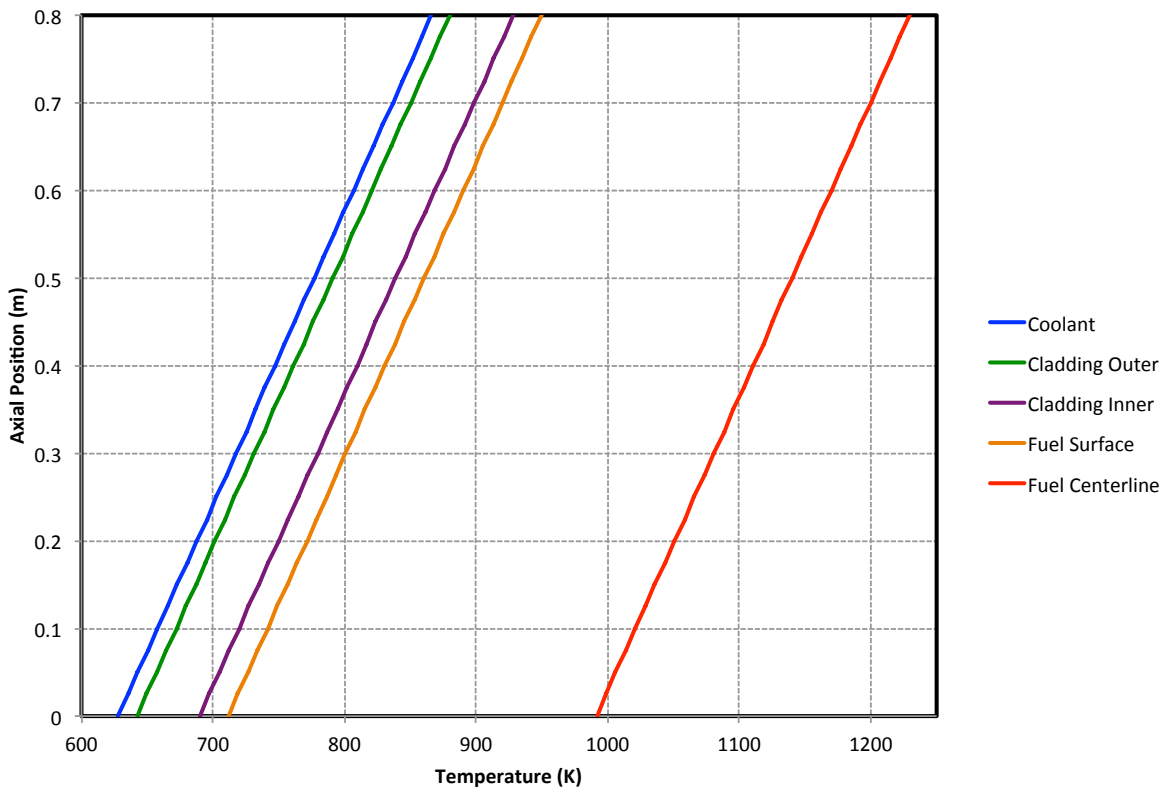

Figure 3.2. Axial Temperature Profile for 50% Power Increase

3.2.3 *Increased Core Inlet Temperature*

In this test case, the core inlet temperature increases by 100 K from 628.15 K to 728.15 K shortly after the start of the simulation. Because all material properties are temperature-independent, the resulting equilibrium temperatures should be exactly 100 K higher than those given in Table 2.1. Therefore, Table 2.1 can be used as a reference for the results if 100 K is added to all temperature values.

3.2.4 *Decreased Sodium Mass Flow Rate*

In this case, the coolant flow rate for the single pin decreases by 50% from 0.150 kg/s to 0.075 kg/s shortly after the start of the simulation. Because the material properties are all temperature-independent, the difference between all temperatures and the core inlet temperature should be exactly twice as large once the system has reached a new equilibrium. Those temperatures are given in Table 3.4 below.

Table 3.4. Temperatures following 50% decrease in coolant flow rate

Axial Position (m)	Coolant Temperature (K)	Cladding Outer Temperature (K)	Cladding Inner Temperature	Fuel Surface Temperature (K)	Fuel Centerline Temperature (K)
0.80	945.610	954.936	986.903	1001.286	1187.796
0.75	925.769	935.095	967.062	981.445	1167.954
0.70	905.928	915.253	947.221	961.604	1148.113
0.65	886.087	895.412	927.380	941.762	1128.272
0.60	866.245	875.571	907.538	921.921	1108.431
0.55	846.404	855.729	887.697	902.080	1088.589
0.50	826.563	835.888	867.856	882.238	1068.748
0.45	806.721	816.047	848.015	862.397	1048.907
0.40	786.880	796.206	828.173	842.556	1029.066
0.35	767.039	776.364	808.332	822.715	1009.224
0.30	747.198	756.523	788.491	802.873	989.383
0.25	727.356	736.682	768.649	783.032	969.542
0.20	707.515	716.841	748.808	763.191	949.701
0.15	687.674	696.999	728.967	743.350	929.859
0.10	667.833	677.158	709.126	723.508	910.018
0.05	647.991	657.317	689.284	703.667	890.177
0.00	628.150	637.475	669.443	683.826	870.335

3.3 Temperature-dependent Material Properties

This group of test cases introduces temperature dependence to a few material properties. The properties that were chosen (sodium heat capacity, cladding thermal conductivity, and fuel thermal conductivity) affect the steady-state temperatures. Because only steady-state analytical solutions have been generated, properties that would affect only the transient results, such as fuel heat capacity, have not been modified.

Analytical axial temperature solutions for each of the three cases below have been created using a solution method similar to the base case solution. For brevity, these analytical solutions are not given below but are available.

3.3.1 Sodium Heat Capacity

In this test case, the heat capacity of the coolant is updated from a constant value of $1260\frac{J}{kg-K}$ to:

$$c_p(T) = 1500 + 0.1\,T \tag{3.1}$$

where temperature is in Kelvin and c_p is in $\frac{J}{kg-K}$. Properties for fuel and cladding remain constant at the values given in Table 2.1. Therefore, the radial ΔT across the cladding, gap, and fuel are the same as for the base case, although the absolute temperatures have changed according to the changes in coolant temperature.

3.3.2 *Cladding Thermal Conductivity*

In this case, the thermal conductivity of the cladding is updated from a constant value of $24\frac{W}{m-K}$ to:

$$k_{\text{clad}}(T) = \frac{3}{100} \times T + 2 \tag{3.1}$$

where temperature is in Kelvin and k_{clad} is in $\frac{W}{m-K}$. The resulting axial temperature profile is given in Table 3.6. Properties for coolant and fuel remain constant at the values given in Table 2.1. Therefore, the radial ΔT from the coolant to the cladding outer surface, across the cladding, and across the gap are the same as for the base case.

3.3.3 *Fuel Thermal Conductivity*

In this case, the thermal conductivity of the fuel is updated from a constant value of $16\frac{W}{m-K}$ to:

$$k_{\text{fuel}}(T) = \frac{T}{100} + 7 \tag{3.1}$$

where temperature is in Kelvin and k_{fuel} is in $\frac{W}{m-K}$. The resulting axial temperature profile is given in Table 3.7. Properties for coolant and cladding remain constant at the values given in Table 2.1. Therefore, the radial ΔT from the coolant to the cladding outer surface, across the gap, and across the fuel are the same as for the base case.

3.4 Neutron Kinetics Cases

Up to this point, total power has been specified for each test. Neutron kinetics solvers are often a part of systems analysis tools. In this section, two simple tests are defined to test steady-state and transient neutron kinetics solvers.

3.4.1 *Delayed Neutron Precursors*

In this test a simple point kinetics model with six delayed neutron precursor groups is added to the definition of the base case. Table 3.5 gives the point kinetics parameters $\beta_{eff,i}$ (effective delayed neutron fraction) and λ_i (decay constant) for each of the groups. The prompt neutron lifetime is defined as 2.0×10^{-7} seconds. For a steady-state problem (i.e. reactivity changes are zero) the steady-state temperature profile throughout the fuel pin should be identical to the temperatures given in Table 2.2. Temperatures calculated during a null-transient simulation should also be compared to the base case temperatures to confirm that the systems analysis code is able to maintain the correct solution.

Table 3.5. Six-Group Delayed Neutron Parameters

Group	$\beta_{eff,i}$	λ_i (1/s)
1	2.0×10^{-4}	1.0×10^{-2}
2	1.0×10^{-3}	3.0×10^{-2}
3	1.0×10^{-3}	1.0×10^{-1}
4	2.5×10^{-3}	3.0×10^{-1}
5	1.5×10^{-3}	8.0×10^{-1}
6	5.0×10^{-4}	3.0

3.4.2 *External Reactivity Insertion*

As an extension to the previous case, this case adds an external reactivity insertion. After 10 seconds of zero reactivity, a step reactivity insertion of \$0.001 is introduced. At 20 seconds, the reactivity drops back to zero. An exact analytical solution to the full point kinetics equations is difficult to obtain, so the prompt jump approximation was used to calculate the resulting power profile based on the point kinetics parameters given in the previous case. The power profile is illustrated in Figure 3.3.

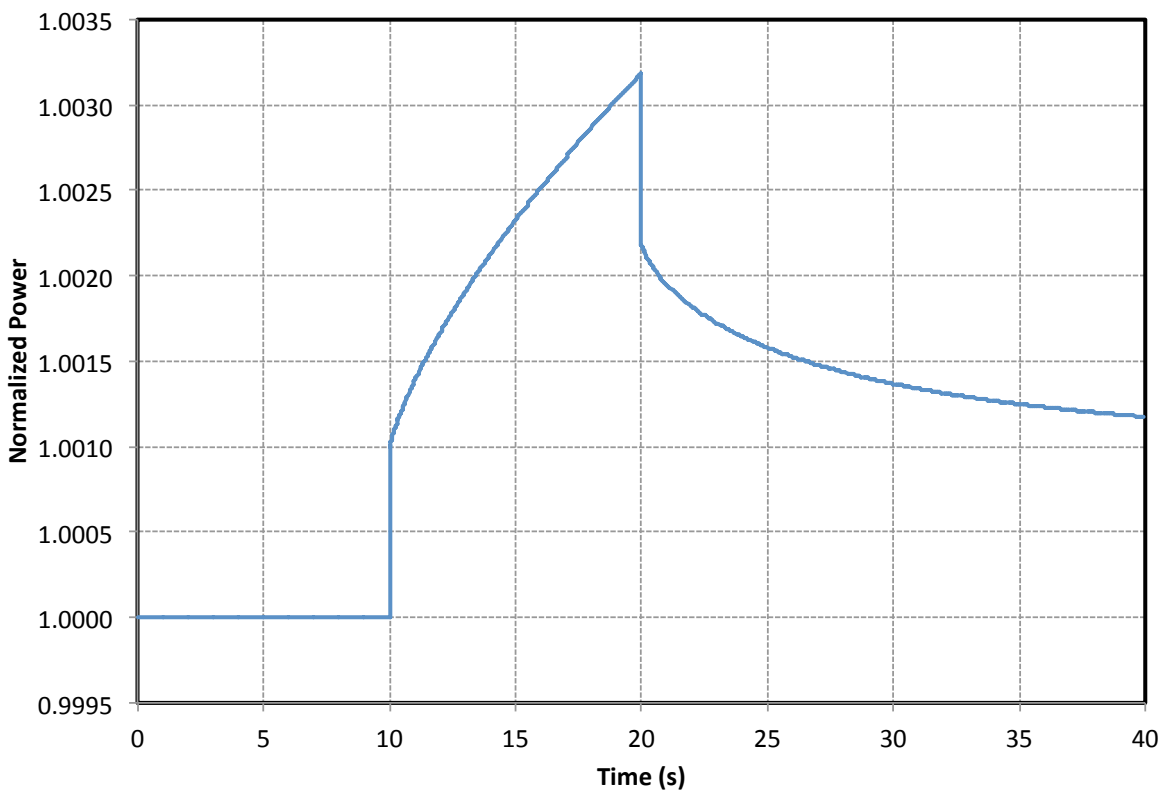

Figure 3.3. \$0.001 Reactivity Insertion for Ten Seconds

Because the reactivity insertion is very small, the prompt jump approximation is considered acceptable and should be sufficient in place of the full analytical solution for comparison against code predictions. Even though this is an analytical approximation, the reference solution can still be used to identify errors to code updates. If results from this test deviate from a previously calculated solution, code developers will quickly know that recent code modifications have led to the different results. It will then be up to the code developers to determine if the different results are intended or unintended.

4 Results of Verification Testing

Many of the test cases described above have been evaluated with two systems analysis codes: M-SFR [2] and SAS4A/SASSYS-1 [4]. In this report, M-SFR refers to the MOOSE-based SFR component model development being carried out as part of the collaboration on RELAP-7 development. RELAP-7 uses the MOOSE object oriented framework to interface with libMesh and PETSc to provide the underlying mesh managements and numerical schemes, while RELAP-7 itself focuses on physical component model developments that represent typical components and systems in a light water reactor (LWR). In collaboration with the developments on RELAP-7, additional developments are being made on both physics modeling and components and systems design that represent typical features of SFRs.

SAS4A/SASSYS-1 was developed at Argonne for thermal, hydraulic, and neutronic analysis of sodium cooled fast reactors. It is used for analysis of safety margins during design basis accidents as well as for severe core disruption accidents with coolant boiling and fuel melting and relocation. While the tests discussed below focus on core thermal-hydraulics, future tests will address the models for point kinetics, reactivity feedbacks, and primary and intermediate loop thermal-hydraulics.

The results of these tests cases for SAS4A/SASSYS-1 and M-SFR are described below. Because the M-SFR components are still under development, not all of the test cases could be evaluated with that capability.

4.1 Base case

The base case, defined in Section 2.1, is a steady-state single-pin problem with constant material properties, dimensions and linear heat generation rate. Figure 4.1 illustrates the coolant pressures calculated by SAS4A/SASSYS-1 and M-SFR for this test as well as the relative differences between the calculated results and the analytical solution. Both codes were able to predict the coolant pressure distribution nearly perfectly. The less than 0.02% difference between the analytical solution and SAS4A/SASSYS-1 results is due to the number of significant digits printed by SAS4A/SASSYS-1 in the output file.

Figures 4.2 and 4.3 illustrate the coolant and cladding outer surface axial temperature profiles, respectively, predicted by SAS4A/SASSYS-1 and M-SFR. Both codes obtain the same coolant and cladding outer surface temperatures as the analytical solution.

Figure 4.4 illustrates the cladding inner axial temperature profile. Both codes predict a ΔT across the cladding that is 0.013 K smaller than the analytical solution at all axial locations. Figure 4.5 illustrates the fuel surface axial temperature profile predicted by both codes. SAS4A/SASSYS-1 calculates the same temperature increase across the gap as the analytical

solution; consequently, the SAS4A/SASSYS-1 fuel surface temperatures are 0.013 K smaller than the analytical temperatures. M-SFR calculates a temperature rise across the gap that is 1.013 K (0.15 %) smaller than the analytical solution. This difference may be related to differences in the predicted fuel centerline temperature, which will be discussed later.

The predicted fuel centerline temperatures are illustrated in Figure 4.4. SAS4A/SASSYS-1 results are again 0.013 K less than the analytical solution; this difference is due to the slightly smaller temperature increase across the cladding.

The ΔT across the fuel that the M-SFR components predict is 1.143 K less than the analytical solution, resulting in a centerline temperature profile that is 2.182 K (0.25%) less than the analytical solution. This difference is due to the use of linear finite elements to solve the heat conduction equation although the temperature distribution is actually quadratic. Consequently, the zero temperature gradient boundary condition that is enforced between the centerline node and the first adjacent node results in an artificially flat temperature profile. This can be improved in the future by using higher order numerical schemes or non-uniform nodalization.

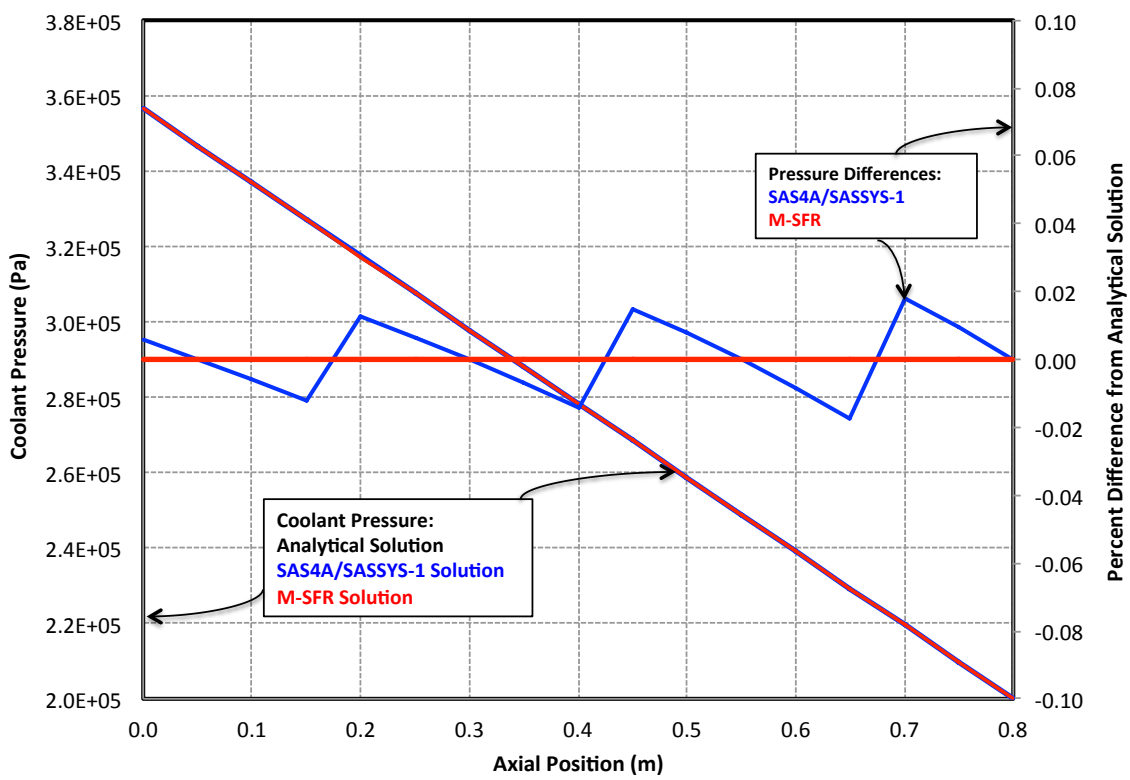

Figure 4.1. Axial coolant pressure distribution for the base case

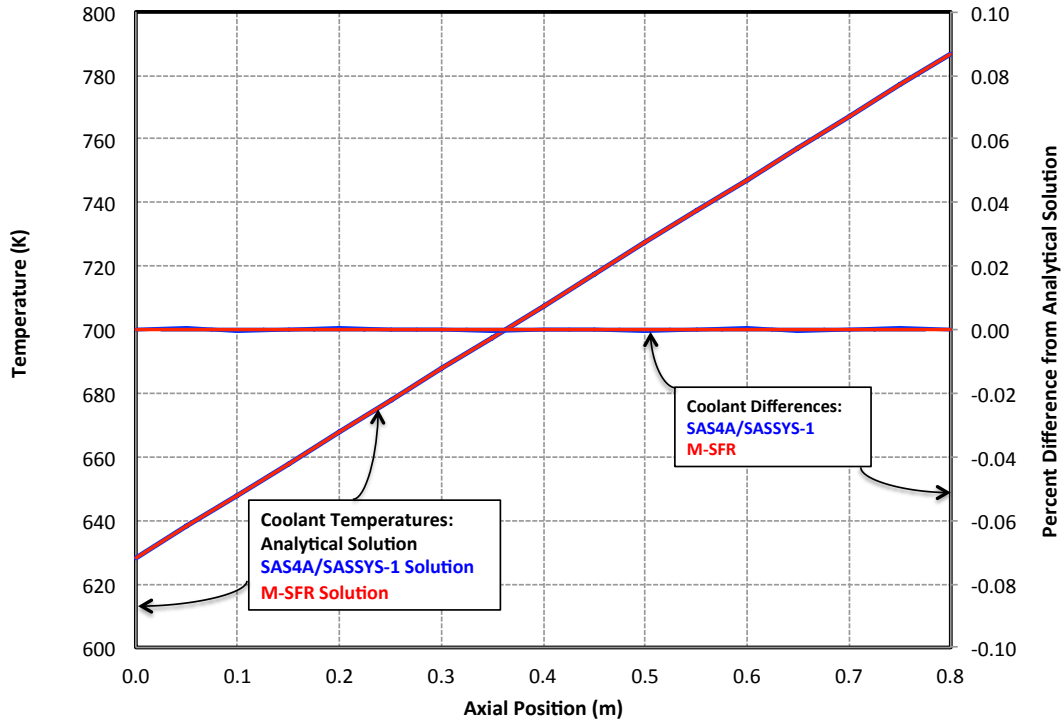

Figure 4.2. Coolant axial temperature distribution for the base case

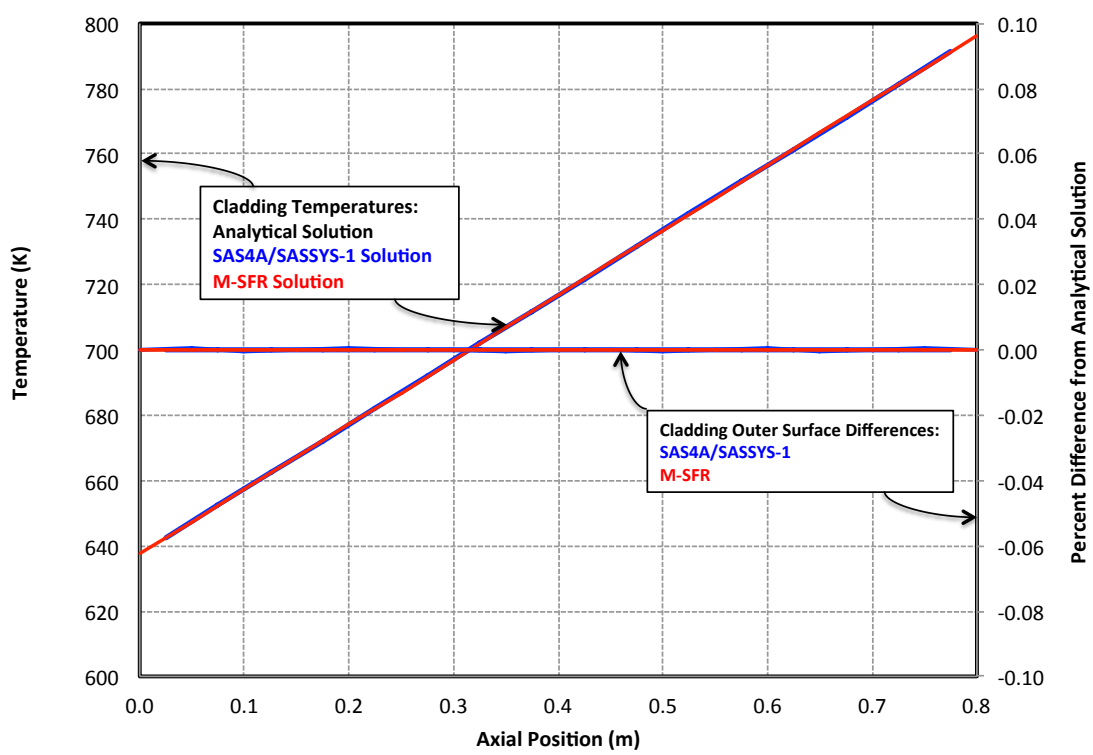

Figure 4.3. Cladding outer surface axial temperature distribution for the base case

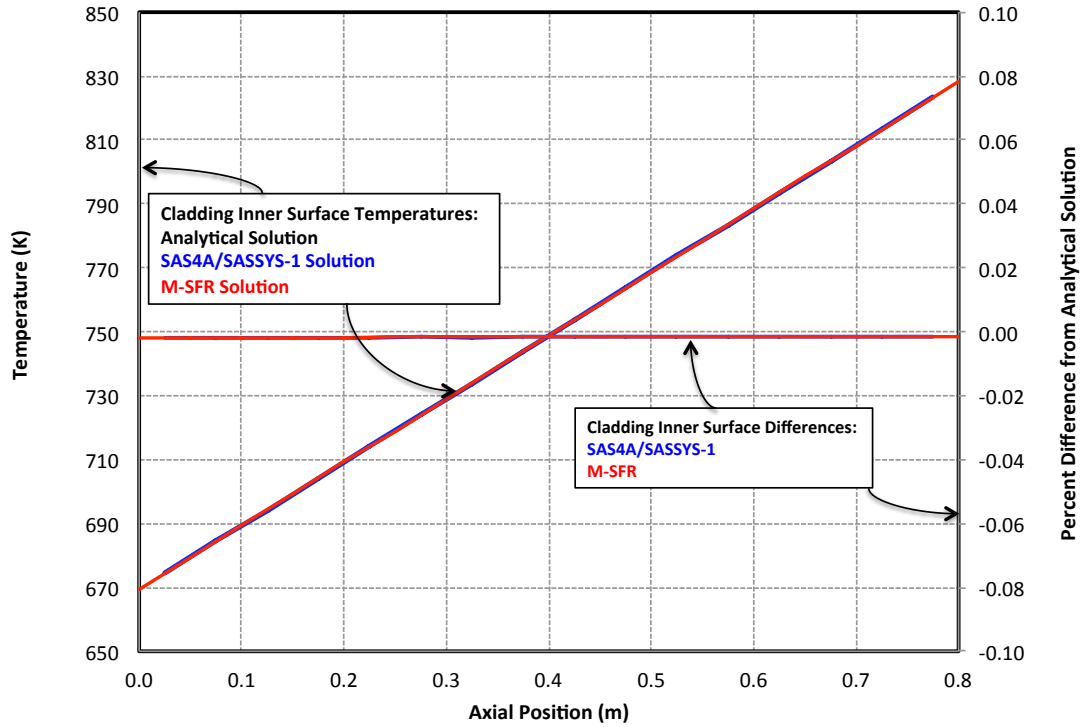

Figure 4.4. Cladding inner surface axial temperature distribution for the base case

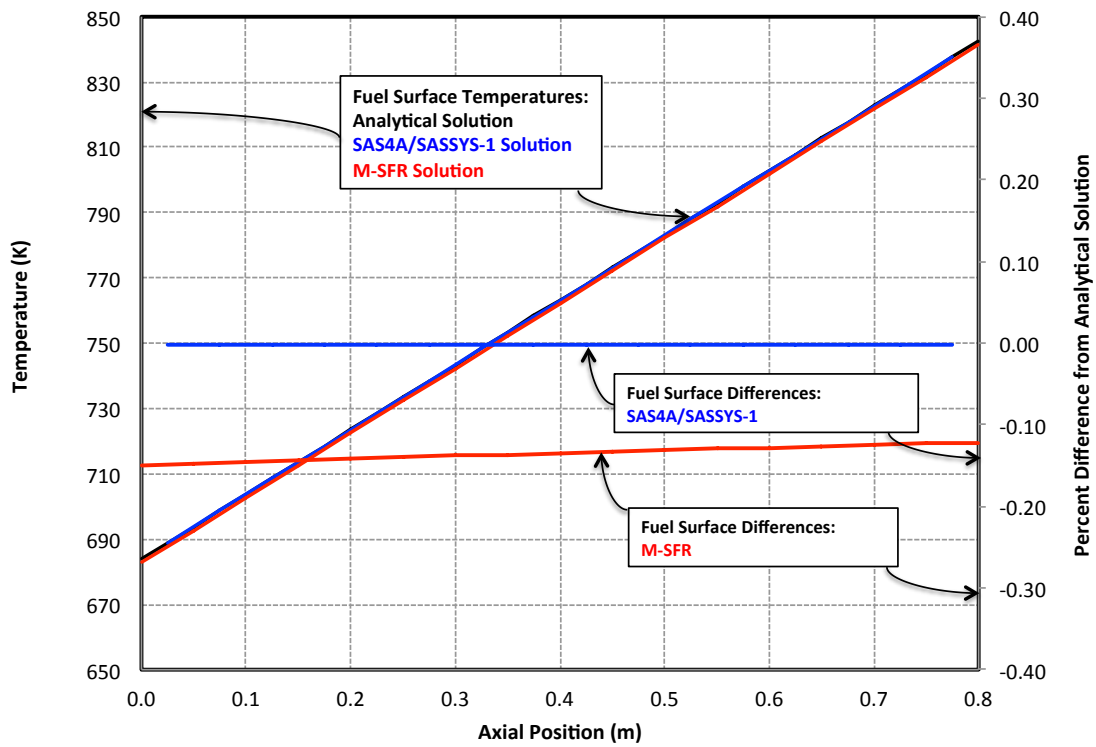

Figure 4.5. Fuel surface axial temperature distribution for the base case

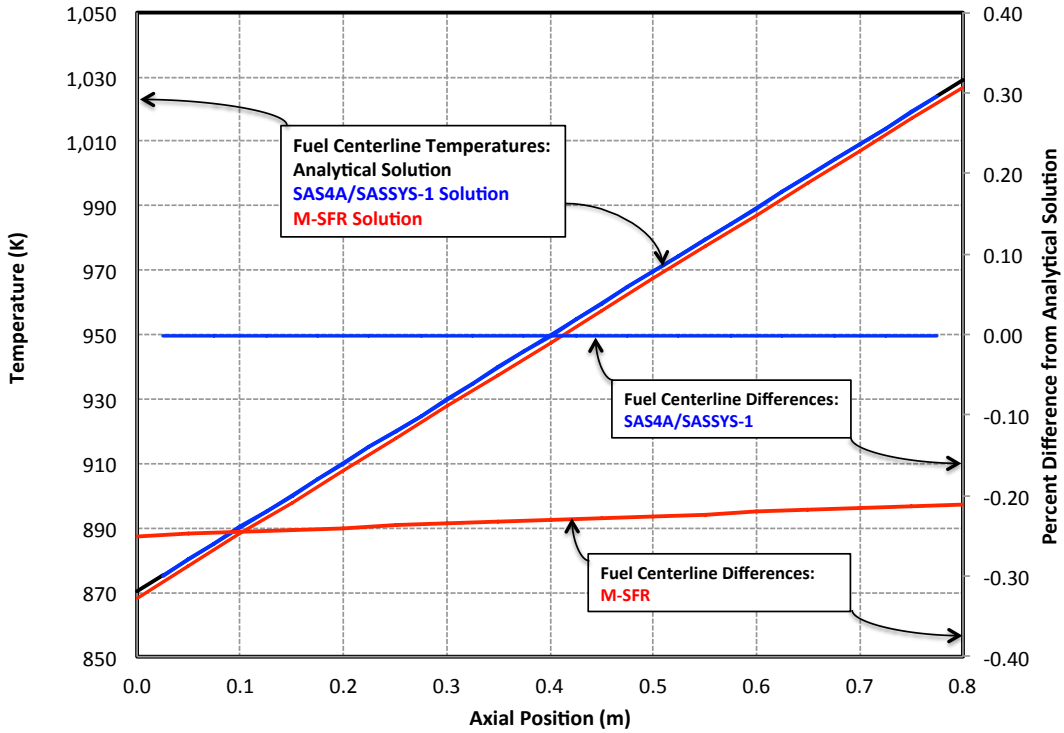

Figure 4.6. Fuel centerline axial temperature distribution for the base case

4.2 Additional Test Case Results

Following the base case evaluations with SAS4A/SASSYS-1 and M-SFR, the tests described in Section 3 were evaluated with both codes and the results for temperature have been compared with the analytical solutions.

4.2.1 Simple Base Case Extensions

The test defined in Section 3.1.1 increases the number of fuel pins from 1 to 91 and the total power from 30 kW to 2730 kW. Both SAS4A/SASSYS-1 and M-SFR obtained the exact same temperatures that were calculated for the base case. The test in Section 3.1.2 increases the number of subassemblies to 100 and the power to 273 MW. Both codes obtained the exact same temperatures as for the base case.

The test defined in Section 3.1.3 added a second channel with different power and flow to the original base case. This test was only performed with SAS4A/SASSYS-1. The results from the SAS4A/SASSYS-1 calculation for the second channel match the analytical solution with the same level of accuracy as for the base case. That is, the largest difference between the simulated temperatures and the analytical temperatures was 0.018 K. Additionally, the temperatures calculated in the unchanged first channel remained unchanged from the base case solution.

The next set of tests, which are given in Sections 3.1.4 and 3.1.5, introduce axial reflectors and fission gas plena above and below the core. For all of these cases, SAS4A/SASSYS-1 correctly calculated the temperature of the new structure below the core at the coolant inlet

temperature of 628.15 K and the temperature of the new structure above the core at the coolant outlet temperature of 786.88 K. Additionally, the temperatures in the fueled region remained unchanged from the base case solution. These tests were not performed with M-SFR.

4.2.2 *Simple Transient Cases*

For the test described in Section 3.2.1, systems analysis codes must maintain the steady-state solution for an extended simulation time when test conditions are unchanged. Both SAS4A/SASSYS-1 and M-SFR correctly maintain the same solution from the base case throughout the entire 1000 seconds.

The three tests described in Sections 3.2.2-3.2.4 are simple transients designed to test the ability of a systems analysis code to re-equilibrate following some change. Each test begins at the conditions of the base case and introduces either an increase in reactor power by 50%, an increase in core inlet temperature by 100 K, or a decrease in core flow rate by 50%. Each test was performed with SAS4A/SASSYS-1 and M-SFR.

The resulting equilibrium temperatures calculated by SAS4A/SASSYS-1 have the same accuracy as for the base case. For a power increase of 50%, the new temperatures are at most 0.032 K different from the analytical solution temperatures. For an inlet temperature increase of 100 K, the new equilibrium temperatures are exactly 100 K higher than for the base case. Consequently, the maximum difference is still 0.013 K. And for a decrease in flow rate from 0.150 kg/s to 0.075 kg/s, the new temperatures calculated by SAS4A/SASSYS-1 are at most 0.013 K different from the analytical temperatures.

The differences between the new equilibrium temperatures calculated by M-SFR and the analytical solutions for these transients are also very similar to the differences for the base case. For the power increase of 50%, the maximum difference in temperature increases from the base case value of 2.182 K to 3.272 K at the fuel centerline. The resulting maximum difference between the M-SFR and analytical results is still 2.182 K for the 100 K coolant inlet temperature increase. For the third transient, a decrease in flow rate of 50%, the M-SFR fuel ΔT and gap ΔT are 2.186 K and 1.026 K, respectively, different from the analytical results.

4.2.3 *Material Property Cases*

The three tests described in Section 3.3 modify the material properties used in the base case. In the first test, a temperature-dependent sodium heat capacity is used. The second test uses a temperature-dependent cladding thermal conductivity. The third test uses a temperature-dependent fuel thermal conductivity. Both codes were used for the fuel thermal conductivity test. Only SAS4A/SASSYS-1 was used for the other two tests.

By introducing a temperature dependent sodium heat capacity, the sodium temperature profile will change but the increases in temperature across the cladding, gap, and fuel should remain unchanged. For this test, the new sodium temperature profile calculated by SAS4A/SASSYS-1 is 0.001 K less than the analytical solutions. The same temperature increases across the cladding, gap, and fuel were calculated by SAS4A/SASSYS-1 so those temperatures are now 0.014 K less than the analytical solution.

Changing the properties of the cladding only affects the temperature increase across the cladding. With the new temperature-dependent cladding thermal conductivity, the temperature increase calculated by SAS4A/SASSYS-1 is 0.010 K less than the analytical solution. The temperature increases from the coolant to the cladding outer surface, across the gap, and from fuel surface to fuel centerline are the same as for the base case.

In the third material property test, a temperature-dependent fuel thermal conductivity is introduced. SAS4A/SASSYS-1 had previously calculated the same increase in temperature across the fuel for the other tests. But for a temperature-dependent thermal conductivity, a maximum difference of 0.031 K is introduced. This error is a function of the nodalization scheme used by SAS4A/SASSYS-1. M-SFR calculates similar errors for this test as it does for the base case. In this case, the difference between the analytical and M-SFR fuel centerline temperatures varies from 2.032 K at the core inlet to 1.966 K at the core outlet.

4.2.4 *Neutron Kinetics Cases*

The test described in Section 3.4.1 introduces a six delayed neutron group point kinetics model to the base case at steady-state. Systems analysis codes with neutron kinetics solvers should be able to calculate and maintain the specified power level as well as the power distribution. For the point kinetics parameters given for this test, SAS4A/SASSYS-1 was able to predict the exact same power level, power distribution, and therefore temperatures at steady-state and throughout a 1000 second simulation. Because M-SFR does not yet have a point kinetics solver, it was not used for this test.

In Section 3.4.2, a simple $0.001 reactivity insertion and removal was defined. Figure 4.5 below illustrates the results found using the prompt jump approximation and SAS4A/SASSYS-1. The two power profiles agree very well for this test. The largest differences occur when the reactivity is inserted at 10 seconds and then removed at 20 seconds. This difference peaks at 0.0008 % and is a function of how the step reactivity insertion/removal is treated by the two methods.

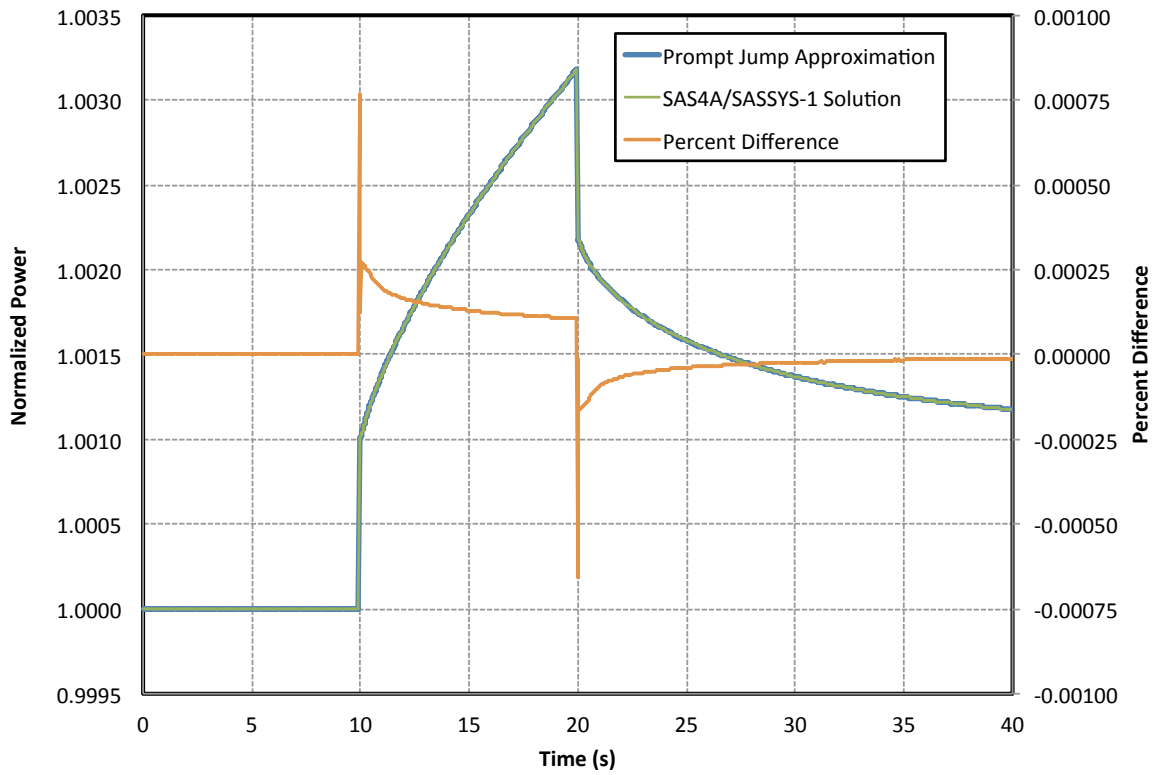

Figure 4.5. Prompt Jump and SAS4A/SASSYS-1 Power Profiles for $0.001 Reactivity Insertion and Removal

5 Future Test Cases

The tests described in this report focus on fuel pin modeling inside the core. Below, additional types of tests are described that would address other areas of a reactor. These types of tests will be developed in the future to expand the verification test suite.

5.1 Neutronics Tests

For each of the tests described above, either power or total reactivity was specified. Additional test cases should be created that test individual reactivity feedback effects. Full analytical solutions may not be practical or possible for these tests so analytical approximations will be created for comparison with code predictions.

In addition to testing the reactivity feedback effects, decay heat modeling will also be tested. The ANS decay heat standard includes tables of decay heat power as a function of time after shutdown following a steady-state irradiation of 10^{13} seconds for four isotopes, U^{235}, U^{238}, Pu^{239}, and Pu^{241}. A systems level decay heat model should be able to predict the results published in the standards.

5.2 Multi-Channel Test

A multi-core-channel test case will be developed to verify the correct flow distribution among multiple core channels with different inlet orifice coefficients and power levels. All

channels will be connected at the bottom and top plena, with known inlet and outlet plena pressure and total inlet mass flow. The flow rates and temperature profiles for each channel calculated by a systems analysis code would then be compared with an analytical solution.

5.3 Component Tests

While most test cases described in Section 3 have been developed to verify the core modeling, additional test cases for other components are necessary to accurately simulate the primary loop and the whole plant of a SFR system. Additional test cases need to be developed to verify the correct modeling of individual components such as pipes, pumps, heat exchangers, and pools. For example, given a set of initial conditions, systems analysis codes should be able to accurately predict the temperature, flow, and pressure throughout a pipe. Similar to the simple core transient tests, each component should be tested independently to isolate code features.

Additional component tests will be developed for additional components needed for the balance of plant and the control systems.

5.4 Simple Loop Test

A simple loop test case will be developed to verify the correct pressure and flow distribution across multiple components with a given pump head. In the event that analytical solutions are too difficult to obtain, engineered hand calculations will be created for direct comparison with code predictions.

The simple loop test case can also be extended for modeling natural circulation flow with zero pump head. The steady-state natural circulation flow rate can be compared with an analytical solution.

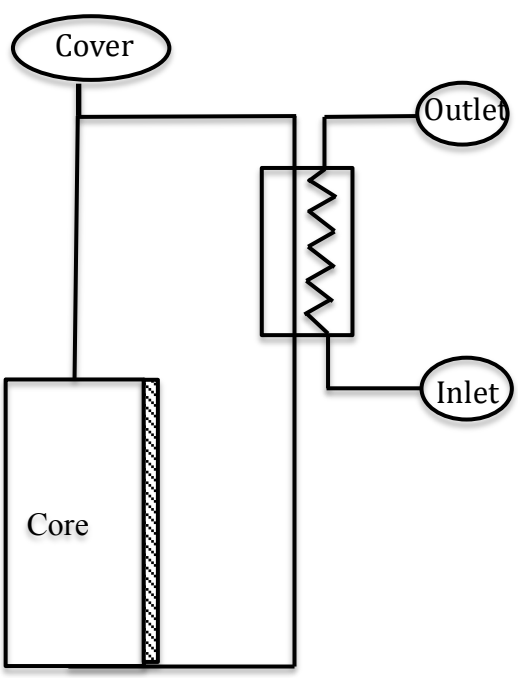

Figure 5.1. Schematics of a test natural circulation loop

5.5 Full System Tests

A test will be developed to verify that systems analysis codes are able to predict the steady-state operating conditions throughout the system of a reference SFR model such as the Advanced Burner Test Reactor [5]. In addition to confirming the steady-state solution, the effects of this coupling core thermal-hydraulic models with models for neutronics and primary/intermediate sodium components can be examined. Existing transient test cases can be identified and further developed. Ideally these transient cases can be based on standard problems from IAEA benchmarks such as the EBR-II shutdown tests.

6 Summary

A suite of test problems has been developed for sodium fast reactor systems analysis that will be used for code verification. A test suite of this nature is important for software quality assurance purposes. Analytical solutions to many of the tests have been provided to confirm code predictions. Several other tests have been created that have numerical solutions when full analytical solutions are not available.

The test cases described in this report were simulated with two systems analysis codes. SAS4A/SASSYS-1 is an existing well-documented sodium fast reactor analysis tool. For SAS4A/SASSYS-1, this test suite is important to confirm that results are not changing during code maintenance. Results from the test cases evaluated with SAS4A/SASSYS-1 compared very well with the analytical and numerical solutions, with maximum temperature differences on the order of 0.013 K for each test.

The Moose-based sodium fast reactor component models are currently being developed as part of a collaboration in the development of RELAP-7 and thus require frequent checks to confirm that updates to the code are not causing unintended changes elsewhere. M-SFR predictions for the test suite cases also compared well to the analytical results. The biggest differences were in fuel-cladding gap and fuel centerline temperatures. Differences were on the order of 2 K. For the fuel centerline temperatures, the error was due to the use of a linear finite element method to solve the heat conduction equation. Future updates to the code will likely improve this approximation. Additional cases will be tested with M-SFR as the code capabilities continue to evolve.

The tests that have been completed focus on calculating fuel and cladding temperature and coolant temperature and pressure. This effort will continue as the tests described above are expanded to address other areas of systems analyses. These will include the primary and intermediate cooling systems and balance of plant. Additionally, more complicated tests will be created that simulate full system transients based loosely on documented fast reactor designs. Furthermore, challenge problems for individual physics phenomena (steep gradient problems, thermal stratified flow, natural circulation instability, etc.) will be developed along with the derived analytical solutions. As it evolves, this test suite will cover the full range of sodium fast reactor conditions including challenging coupled multi-physics challenge problems.

REFERENCES

[1] D. Anders, R. Berry, D. Gaston, et al., "Demonstration of a Steady State Single Phase PWR Simulation with RELAP-7", INL/EXT-12-25924, May 2012.

[2] R. Hu and T. H. Fanning, Argonne National Laboratory, unpublished information, August 31, 2012.

[3] Todreas, N. E. and Kazimi, M. S., Nuclear Systems II: Elements Of Thermal Design. Reading, Massachusetts: Taylor & Francis, 1990.

[4] T. H. Fanning, ed., The SAS4A/SASSYS-1 Safety Analysis Code System, Argonne National Laboratory, ANL/NE-12/4, January 31, 2012.

[5] Y. I. Chang, P. J. Finck, and C. Grandy, "Advanced Burner Test Reactor, Preconceptual Design Report," ANL-ABR-1 (ANL-AFCI-173), Argonne National Laboratory, Sept. 2006.

Nuclear Engineering Division
Argonne National Laboratory
9700 South Cass Avenue
Argonne, IL 60439

www.anl.gov